Voltage-driven alterations to neuron viscoelasticity

Celine Kayal[a,b,*], Casey Adam[a,b,*], Miren Tamayo-Elizalde[a,b], Hua Ye[a,b], Antoine Jerusalem[a,*]

[a]*Department of Engineering Science, University of Oxford,Oxford, OX1 3JP, UK*
[b]*Institute of Biomedical Engineering, University of Oxford, Oxford, OX3 7DQ*

Abstract

The consideration of neurons as coupled mechanical-electrophysiological systems is supported by a growing body of experimental evidence, including observations that cell membranes mechanically deform during the propagation of an action potential. However, the short-term (seconds to minutes) influence of membrane voltage on the mechanical properties of a neuron at the single-cell level remains unknown. Here, we use microscale dynamic mechanical analysis to demonstrate that changes in membrane potential induce changes in the mechanical properties of individual neurons. We simultaneously measured the membrane potential and mechanical properties of individual neurons via a multiphysics single-cell setup. Membrane voltage of a single neuron was measured via whole cell patch clamp. The mechanical properties of the same neuron were measured via a nanoindenter, which applied a dynamic indentation to the neuron at different frequencies. Neuronal storage and loss modului were lower for positive voltages than negative voltages. The observed effects of membrane voltage on neuron mechanics could be due to piezoelectric or flexoelectric effects and altered ion distributions under the applied voltage. Such effects could change cell mechanics by changing the intermolecular interactions between ions and the various biomolecules within the membrane and cytoskeleton.

Keywords: Mechanical-electrophysiological coupling | Neuron | Nanoindentation | Patch clamp

*Corresponding authors
Email addresses: celine.kayal@ucl.ac.uk (Celine Kayal), casey.adam@sjc.ox.ac.uk (Casey Adam), antoine.jerusalem@eng.ox.ac.uk (Antoine Jerusalem)

Introduction

Changes in neuronal membrane voltage above a given depolarisation threshold induce the generation and propagation of action potentials (APs). This electrical activity is directly related to the flow of ions across the membrane through the opening and closing of transmembrane ion channels. In addition to their electrophysiological function, ion channels also regulate cell volume [1] and provide mechanosensitive functions [2, 3]. For example, mechanical forces can trigger electrophysiological and biochemical responses in cells by directly affecting the activity of mechanosensitive ion channels [4]. Conversely, the propagation of APs has also been shown to induce physical and structural changes at the cell scale such as membrane deformation and displacement, or nerve thickness variation [5, 6, 7, 8, 9, 10]. The action of ion channels also directly depends on the surrounding membrane structure [11]. Together, these observations suggest a close relationship between neuronal electrophysiology and mechanics [12].

Over the past decades, new techniques and methodologies have been developed to measure and quantify the submicroscopic mechanical properties of materials [13, 14]. One such technique is nanoindentation, which can perform quasi-static and/or dynamic loading measurements of the mechanical properties of a sample at the micro- or nanoscale [15]. Using nanoindentation and other micro/nanoscale techniques, an increasing body of work has studied the relationship between a cell's mechanical properties and functionality [16], and demonstrated that the mechanical properties of cells are essential determinants of cellular behavior under normal and pathological conditions [17, 18, 3]. However, relatively few studies account for coupling between the mechanical and electrical properties of cells. While some recent work has proposed the development of novel experimental techniques that enable successful simultaneous measurement of the electrophysiology and mechanical properties of neurons [19, 20], such measurements are still in their infancy. In particular, to the best of our knowledge, no study has measured the impact of membrane electrical potential on neuron mechanics at the single-cell level. To address this issue, we measured how induced membrane potentials (mV) affect the short-term (seconds to minutes) mechanical properties of individual neurons by employing a recently developed multiphysics setup that simultaneously combines whole cell patch clamp, nanoindentation, and

imaging [20].

Materials and Methods

Cell culture

F11 cells (embryonic rat dorsal root ganglion × mouse neuroblastoma (N18TG-2, passage 20-24) hybrid, ECCAC, UK)[21] were seeded at 1×10^5 cells per dish on 50 mm glass bottom petri dishes (glass thickness 1.5 mm, Wilco Wells, Amsterdam, NL) in 2 mL differentiation media (DMEM, 1% foetal bovine serum (FBS), 2 μM retinoic acid, 10 μM IBMX (3-isobutyl-1-mythylxanthine), 0.5% insulin transferrin selenium, 1% penicillin/streptomycin, 50 ng/mL nerve growth factor, 0.5 mM 8-bromoadenosine $3' - 5'$ cyclic monophosphate). Cultures were maintained for 5-8 differentiation days in a humidified incubator (5% CO_2 at 37°C). Every other day, 1 mL of media (Gibco, USA) was replaced by prewarmed (37°C) differentiation media. After 5-8 days of differentiation, cells exhibited traits of mature neurons, such as spontaneous AP firing and neurite elongation [20]. These differentiated cells are established models of sensory neurons [21, 22, 23, 24], with mechanical properties comparable to other neuronal cell types [25].

Dynamic mechanical analysis (DMA)

The mechanical properties of a single cell were measured under compression using a nanoindenter (Chiaro, Optics 11, Amsterdam, NL). Probes (Optics11 Life) consisting of a spherical bead (radius of 8 ± 0.5 μm) [26] attached to a cantilever (stiffness of $0.029 - 0.035$ N/m) were used. Microscale DMA was performed to measure the viscoelastic behavior of F11 cells by quantifying the storage (E') and loss (E'') moduli of the cell. E' accounts for the energy stored elastically, which is recovered after the indentation [27, 28, 29]. E'' accounts for the viscous energy, dissipated as heat, during the indentation [27, 28, 29]. For each measurement, the selected cell was precompressed by 1 μm over a period of 5 s followed by a relaxation of 30 s. DMA was then performed by applying a sinusoidal compression with a displacement amplitude of 400 nm and a specific frequency between 0.5 Hz and 10 Hz. DMA at several frequencies was performed. After measurement at a single frequency, the next measurement was not performed for at least 20 s, to allow for cell relaxation [20]. E' and E'' for each measurement frequency were calculated by the Piuma software by fitting the experimental force and indentation time signals [30].

Electrophysiology

Whole cell patch clamp was performed on a single cell using a Digidata 1550A digitizer acquisition system, pCLAMP 10 data acquisition software, and a Multiclamp 700B MicroElectrode amplifier (Molecular Devices, CA). The intracellular solution contained 140 mM KCl, 5 mM NaCl, 0.1 mM $CaCl_2$, 2 mM $MgCl_2$, 10 mM HEPES, 2 mM ATP, 1 mM GTP and 1mM EGTA with pH adjusted to 7.3 by addition of KOH and osmolarity adjusted to 300 mOsm/L by glucose addition. The extracellular solution contained 130 mM NaCl, 5 mM KCl, 2 mM $CaCl_2$, 1 mM $MgCl_2$, 10 mM glucose, and 10 mM HEPES, and was adjusted to 7.4 pH by NaOH and 310 mOsm/L by glucose addition. All reagents were purchased from Sigma-Aldrich, St. Louis, MO. Patch clamp recording pipettes were pulled from borosilicate glass capillaries (BF100-78-10, Sutter Instruments) by a micropipette puller (Model P-1000, Sutter Instruments), to a resistance of 3-5 MΩ. Pulling parameters were based on previously published work [31]. After a Giga-seal was formed between the pipette and a single cell, suction was applied to rupture the membrane patch and form a whole-cell patch configuration.

Assessment of the electrophysiological-mechanical coupling

Simultaneous measurements of the electrophysiology and mechanical properties of a single F11 cell were performed using the multiphysics setup designed and described by the authors in Ref. [20]. First, the cell was clamped with the patch clamp recording pipette. Next, the cell was indented with the nanoindenter tip, and DMA was performed. The resulting measurement configuration is shown in Fig. 1(A). A specific membrane potential was induced and maintained for the duration of the DMA test. Membrane potential was tracked throughout the experiment to ensure that the quality of the clamp was maintained. If the clamp was lost or damaged, the data were discarded. A minimum of 4 cells were measured at each applied potential in order to account for variability in the results due to factors such as cell size, cell heterogeneity, and spatial position of the clamp and nanoindenter on the cell surface. Measurements were conducted at potentials of: -100 mV (n=4); -50 mV (n=16), -40 mV (n=19), 0 mV (n=18), 10 mV (n=15), 50 mV (n=14), patch without imposed voltage (n=7), and no patch (n=12).

Only mature neurons, with neurites extending from the soma, were measured. Cells with a round soma, at least 20 μm in diameter, were selected so that both the nanoindenter and patch clamp could be applied to the cell without directly touching each other. To minimise effects from neighboring cells,

measurements were only performed on cells whose somas were not in direct contact with those of other neurons. For each nanoindenter measurement, cells were measured at 1 Hz during and after the DMA frequency sweep. If E' and E'' differed between these two measurements, it was assumed that the cell had been damaged during the measurement, and the data for the particular cell were not included in the final analysis.

Microscopy

An inverted microscope Nikon Eclipse Ti (Nikon Instruments Inc., USA) was used to acquire images of F11 cells. Images were captured with 10×, 20× or 40× objectives.

Statistical Analysis

A Shapiro-Wilk test was used to test normality of the data. Differences between measurements were evaluated by performing a one-way ANOVA test followed by a Wilcoxon post hoc test to obtain multiple comparison p values. Comparison p values are mentioned in figure captions.

Results and discussion

A schematic of the multiphysics experimental setup for simultaneous recording of cell mechanics and cell electrophysiology is shown in Fig. 1(A). First, a single F11 cell was clamped. Next, the cell body was indented 1 μm. This indentation depth was within the cell's linear viscoelastic regime [20]. After the initial indentation, oscillatory strains with a 400 nm amplitude were applied at different frequencies (0.5, 1, 2.5, 5, 7.5, and 10 Hz) to perform microscale DMA to measure E' and E'' of the cell in its resting state. Finally, cell E' and E'' were measured at different voltages (-100 mV, -50 mV, -40 mV, 0 mV, 10 mV, and 50 mV) imposed by the clamp. Since the thickness of the cell membrane is 3-10 nm [32], the applied 1 ± 0.4 μm indentations likely deformed intracellular components of the cell in addition to the plasma membrane. Therefore, the measured E' and E'' represent properties arising from the combined membrane, cytoskeleton, and possibly nucleus of the neuron.

Patch clamp induces morphological and functional changes to a cell via pressure/suction on the cell membrane [33], which could potentially affect cell mechanics. To control for these effects, DMA with no imposed electrical potential was performed on individual unclamped (control) and clamped

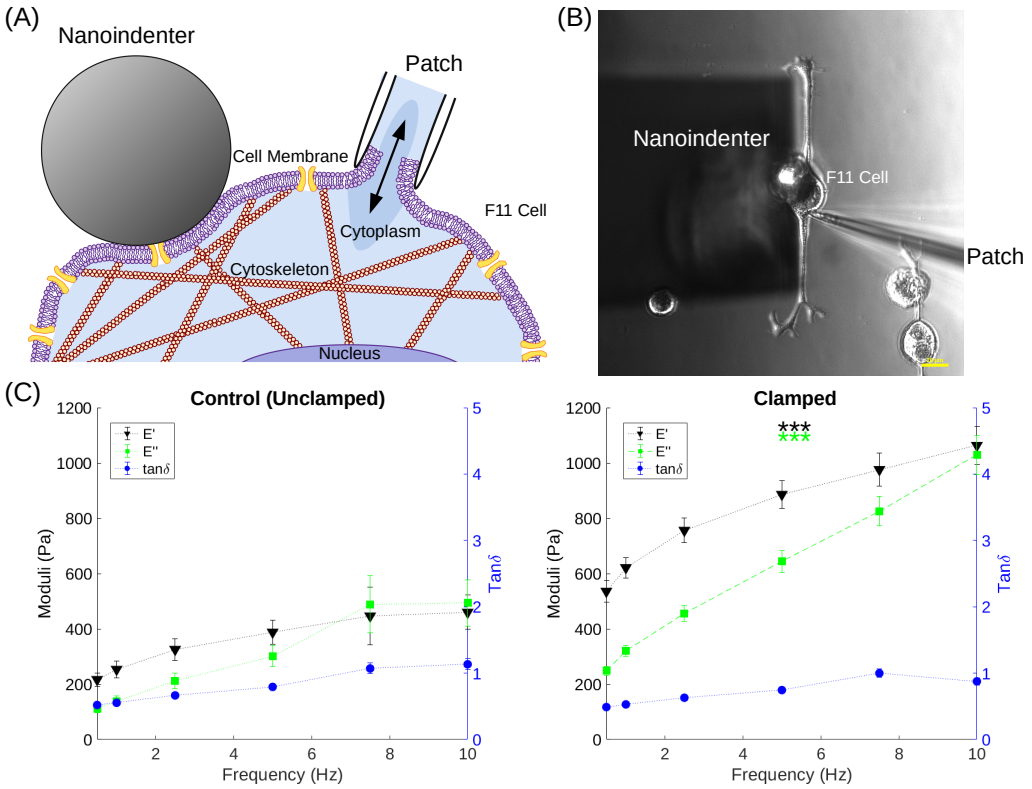

Figure 1: Schematic representation (A) and microscope image (B) of the simultaneous measurement of a single neuron's mechanical properties (via a nanoindenter) and electrophysiology (via whole cell patch clamp), scale bar: 20 μm. (C) Storage and loss moduli (E' and E'', respectively) and tanδ measurements of control (unclamped) and patched cells. $E'\pm$ standard error (SE) (Pa) is shown in black, $E''\pm$ SE (Pa) in green, and $\tan\delta \pm$ SE in blue. Statistical analyses were performed between clamped and control measurements at each frequency. Both E' and E'' were significantly different between clamped and control cells at each frequency, ***p$<$ 0.001.

cells. As shown in Fig. 1(C), both E' and E'' significantly (***p$<$0.001) increased when cells were clamped. For all measured frequencies, the moduli of clamped cells were $\simeq$2$\times$ higher than those of the control (Table 1). Since both E' and E'' increased in a similar manner, the ratio of the two, i.e. the loss tangent $\tan\delta = \frac{E''}{E'}$, was not affected by clamping.

Several possible mechanisms could explain the observed patch clamp effects on cell mechanics. First, deformation of the cell imposed by the patch (illustrated in Fig.1(A)), in addition to that imposed by DMA, could de-

Table 1: Storage modulus (E'), loss modulus (E''), and loss tangent ($\tan\delta = E''/E'$) ± SE at each DMA frequency (f) for neurons without (control) and with patch clamp.

f (Hz)	E' (Pa)		E'' (Pa)		$\tan\delta$	
	Control	Clamped	Control	Clamped	Control	Clamped
0.5	216.95 ± 23.78	535.92 ±38.26	111.73 ±13.96	248.28±16.17	0.52 ± 0.02	0.49 ± 0.03
1	253.72±30.09	621.48±36.97	138.78 ±17.95	320.91 ±18.86	0.55 ± 0.03	0.53 ± 0.03
2.5	325.81 ± 39.07	756.30±43.69	211.90±27.40	455.57± 29.18	0.66 ± 0.04	0.63 ± 0.03
5	388.18± 44.22	886.23 ±50.49	301.72±37.81	643.56± 40.47	0.79 ± 0.05	0.74 ± 0.04
7.5	446.50±104.14	976.08±60.27	488.75 ±102.96	826.08 ±54.20	1.07 ± 0.08	1.00 ± 0.07
10	460.25± 62.25	1063.40±68.29	493.50±83.28	1028.30± 70.43	1.13 ± 0.08	0.88 ± 0.06

form the cell more than the desired 1 ± 0.4 μm, potentially pushing measurements outside the linear viscoelastic regime of the cell. Alternatively, induced membrane curvature by the patch could alter the ion distribution on the membrane [34, 35, 36] or the fluidity of the membrane [37, 38], and thereby alter the mechanical properties of the membrane. Additionally, since the cytoskeleton of the cell is anchored to the membrane, alterations to the membrane by the patch could potentially alter the cytoskeleton dynamics of the neuron, which could result in additional changes to cell mechanics [39].

Next, we studied the influence of membrane potential on cell mechanics by imposing a voltage between -100 mV and 50 mV, and performing DMA at each potential. An example of this procedure is shown in Fig. 2(A). DMA measurements at a given potential were compared to control DMA measurements collected on the patched cell before any membrane potential was imposed. Fig. 2(B) shows E', E'', and $\tan\delta$ at different imposed voltages as a function of frequency (Hz). The values of E' and E'' changed in a similar manner, resulting in a constant $\tan\delta$. These results are reminiscent of those in Fig.1(B).

Fig. 2(C) shows E', E'', and $\tan\delta$ as a function of membrane potential (mV) for each DMA frequency. Both moduli remained constant at potentials between -100 mV and 0 mV. When positive voltage was imposed (at 10 and 50 mV), both E' and E'' decreased. In particular, cell E' and E'' were significantly lower at 50 mV (by a factor $\simeq$1.5; * $p<0.05$) compared to the measurements at -50, -40 and 0 mV. These observations are not due to the effects of the clamp, shown in Fig. 1(B), since the control was the clamped cell before any voltage was applied. Therefore, the results of Fig. 2(B) and 2(C) arise from the different imposed voltages. The trends we observed in E' and E'' with frequency agree with those previously reported at both the cell [20] and tissue [40] level. As with Fig. 1(B), alterations in E' and E''

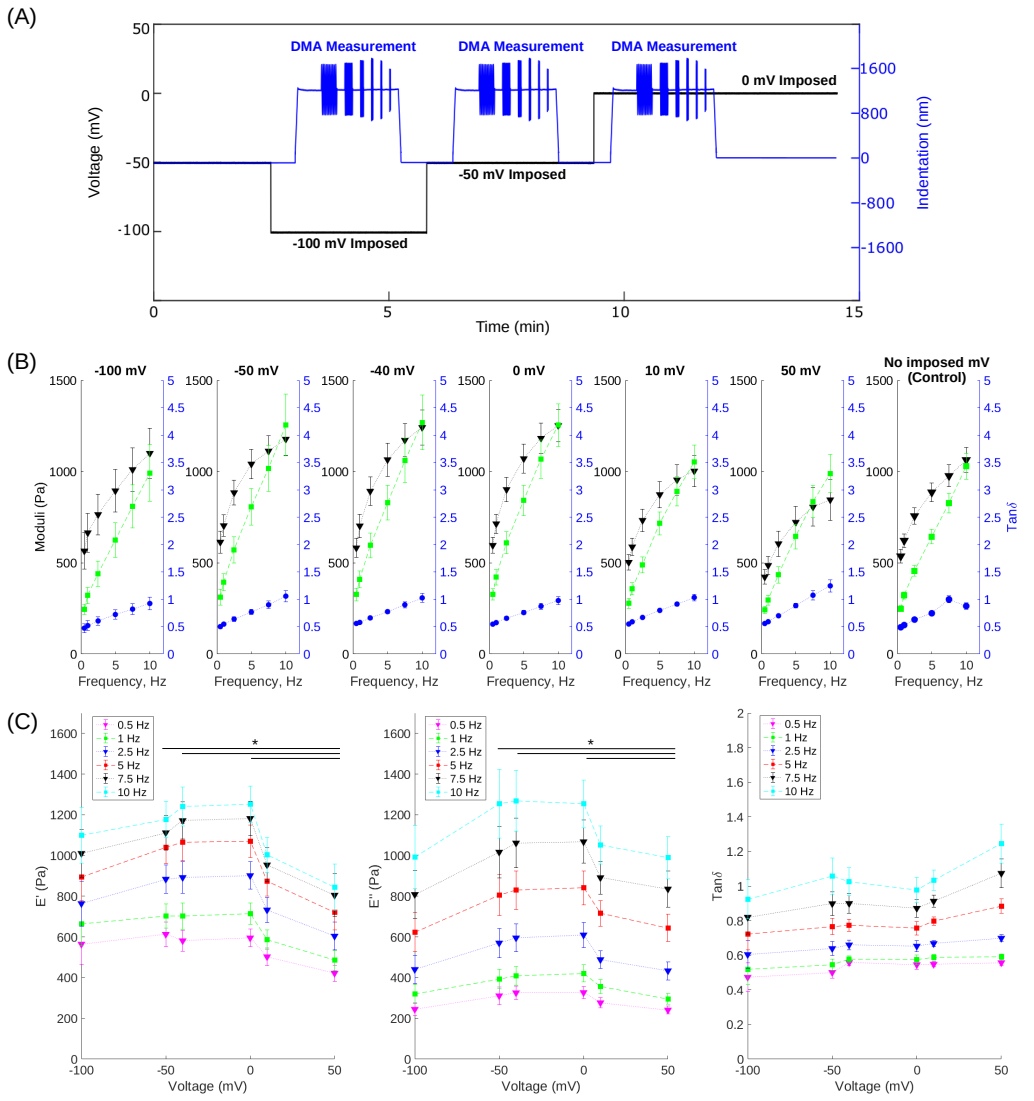

Figure 2: (A) Example multiphysics experiment procedure over a 3.33 min time interval. A voltage is imposed via patch clamp (black, -100, -50 and 0 mV) while DMA (blue) at different frequencies is performed via nanoindentation on the same cell (duration 2.5 min for 6 frequencies). Before time 0, control DMA measurements are performed on the patched cell without any imposed voltage. (B) Frequency dependent variation of storage modulus $E' \pm$ SE (Pa) in black, loss modulus $E'' \pm$ SE (Pa) in green, and the loss tangent $\tan\delta \pm$ SE in blue of neuronal cells for multiple membrane potentials (mV). (C) E' (Pa), E'' (Pa), and $\tan\delta \pm$ SE as a function of membrane potential (mV) for each DMA frequency, n=[4-19]. Statistical analysis was performed between each voltage at a given frequency, * $p<0.05$. Measured $\tan\delta$ were not significantly different.

between positive and negative voltages occurred in a similar manner, thereby resulting in a constant $\tan\delta$ regardless of membrane potential.

Several mechanisms could explain the observed alterations to energy storage and dissipation between positive and negative membrane potentials. For example, imposed voltages alter the activity of channels which regulate cell volume and morphology [41], such as aquaporins [42, 43] and/or ion channels [4]. Alterations to cell morphology via altered channel activity could potentially change the mechanical properties of the cell. Additionally, it is already known that applied voltage alters the spatial distribution of lipids and proteins in the cell membrane, and thereby alters membrane fluidity/state and mechanics [44, 12]. Alterations in the spatial distribution of membrane lipids could also alter lipid polarisation and hence the structure of the cell membrane [45, 46]. Lipid redistribution and membrane structure alterations occur at the microscale, and can alter whole-cell morphology [47, 19]. These alterations to cell morphology could potentially result in altered cell mechanics. It is also reasonable to hypothesise that the imposed voltage affected multiple cellular components, rather than the cell membrane alone. For example, it is already known that alterations to the conformation of the cytoskeleton alter cytoskeletal properties and cell mechanics [39]. The neuronal cytoskeleton consists mainly of actin and spectrin [48]. Actin [49] and spectrin [50] are piezoelectric, meaning they undergo strain when a voltage is applied and vice versa [51]. Therefore, cytoskeletal strains under the voltages imposed in our experiments [51] could potentially alter cytosketal and thereby cellular mechanics. Similarly, the cell membrane is flexoelectric [44], and many components (especially proteins) of the membrane are piezoelectric or exhibit other forms of mechanoelectric coupling [52, 53, 44]. Furthermore, the cytoskeleton is anchored to the cell membrane, and alterations to one component can alter the other [54, 55]. For example, cytoskeletal anchoring to the membrane alters ion channel distribution in the membrane and lipid fluidity [54, 56]. The membrane-cytoskeleton system as a whole determines cell shape and mechanics [57]. Together, these observations suggest that changes in cell mechanics due to different imposed voltages may arise from alterations to the conformation of molecules in the cytoskeleton and membrane via the induced potential. Additionally, the cytoskeleton (and therefore the membrane) is connected to the cell nucleus [58, 59]. Again, DNA and other components of the nucleus are piezoelectric [52, 60, 53]. Changes in the conformation of the nucleus could therefore potentially alter the conformation of the cytoskeleton [58, 59], and thereby the conformation

of the cell membrane, further altering the mechanical properties of the cell. Additional experiments, employing tools such as atomic force microscopy and/or ion channel or cytoskeletal inhibitors, are needed to determine which of the changes proposed in this paragraph contribute most to our results.

Piezoelectric, flexoelectric, and other mechanoelectric behaviors in biological systems arise from the fact that most biomolecules (such as actin, spectrin, DNA, proteins, and lipid heads) are small and charged [53, 61, 28]. Interactions between biomolecule charges and the surrounding water and ions play an important role in modulating the charge, conformation, and mechanical properties of the biomolecule [28, 62]. For example, interaction of membranes with ions alters the fluidity and mechanical properties of the membrane [63, 64, 36]. Hydration of actin and spectrin plays an important role in the mechanical properties and conformation of actin/spectrin cytoskeletons [65]. Ions also have the ability to modulate hydrogen bonds and/or alter covalent interactions (by facilitating reactions or sterically blocking sites where covalent bonds can form) that determine how energy is stored (giving rise to E') and dissipated (giving rise to E'') by the components of a cell [62, 66, 67]. The voltages imposed in these experiments likely alter the distribution (steady state) of ions inside and immediately outside the cell [68]. Such altered ionic distributions could in turn alter imtermolecular interactions [62] and thereby the mechanical properties of the membrane, proteins, cytoskeleton, and other cellular components. Additionally, it is reasonable to hypothesise that sign reversal of the membrane potential (negative to positive) would alter ionic distribution more than changing voltage within either positive or negative ranges (for example from -100 to -50 mV), thereby explaining our observation that the largest change in E' and E'' of the neuron occurred between positive and negative membrane potentials.

Future investigation into neuronal multiphysics should test the validity of the hypothesis that membrane potential affects cell mechanics by altering ion distributions, and consequentially interactions between biomolecules within the neuron. To this end, several different experiments can be performed. For the first experiment, if the ion hypothesis is true, altering extracellular salt concentration should have similar effects to imposed membrane potentials on cell electrophysiology and mechanics. Measurements using our multiphysics setup, with patch clamp measuring the cell's resting potential and nanoindentation performing microscale DMA, could be performed on cells in solutions of various salts and salt concentrations. The second batch of experiments should test the effects of membrane potential on cellular components.

For such studies, atomic force microscope (AFM) cellular imaging techniques [69, 70] could be employed to image and measure the mechanical properties of cells and their intracellular components simultaneously. The effects of voltage on cell mechanics in such AFM experiments could be studied by applying voltage in the AFM [71], or by performing AFM on cells in solutions of different salts or salt concentrations. Similarly, AFM measurements of the mechanical properties of isolated membranes, actin, spectrin, and DNA in different ionic conditions or applied voltages could be performed.

In summary, the objective of this work was to gain insight into electromechanical coupling in neurons by investigating the short-term (seconds to minutes) influence of imposed voltage on neuron mechanics. We found that membrane potential altered neuron viscoelasticity. Similar observations to ours have been reported for cells without patch clamp [72, 20]. However, unlike previous studies, our study also demonstrated a decrease in E' and E'' with positive membrane voltages. The observed effects of applied voltage on neuron mechanics could be due to altered intermolecular and ionic interactions (caused by the imposed voltage) within the cell membrane, cytoskeleton, and possibly cell nucleus. Our observations could have implications for several neuronal processes. Alterations to neuron mechanical properties affect the neuron's ability to generate and propagate APs [12], and could explain the effects of a variety of stimuli on nervous system activity [73, 74, 75, 12]. Therefore, future work designed to test the ion hypothesis proposed here and elucidate the mechanisms behind mechanoelectric coupling in neurons could help explain a variety of phenomena, and increase our understanding of AP propagation in neurons. Such understanding would increase our ability to exploit mechanoelectric coupling in neurons for clinical applications such as ultrasound neuromodulation [12] or the treatment of paralysis [76, 77].

Author Contributions

Author contributions: C.K., M.T.-E. and A.J. designed the research; C.K. performed data collection and analysis; C.A., C.K., and A.J. wrote the paper; H.Y. supervised the experimental work; A.J. supervised the overall research.

Acknowledgments

The authors acknowledge funding from the EPSRC Healthcare Technologies Challenge Award EP/N020987/1.

References

[1] F. Lang, E. Shumilina, M. Ritter, E. Gulbins, A. Vereninov, S. M. Huber, Ion channels and cell volume in regulation of cell proliferation and apoptotic cell death, in: F. Lang (Ed.), Contributions to Nephrology, Publisher: Karger, 2006, pp. 142–160. doi:10.1159/000096321.

[2] A. Anishkin, S. H. Loukin, J. Teng, C. Kung, Feeling the hidden mechanical forces in lipid bilayer is an original sense, PNAS 111 (22) (2014) 7898–7905. doi:https://doi.org/10.1073/pnas.1313364111.

[3] F. Bianchi, M. Malboubi, J. H. George, H. Ye, A. Jerusalem, M. S. Thompson, Ion current and action potential alterations in peripheral neurons subject to uniaxial strain, Journal of Neuroscience Research 97 (7) (2019) 744–751. doi:10.1002/jnr.24408.

[4] S. S. Ranade, R. Syeda, A. Patapoutian, Mechanically activated ion channels, Neuron 87 (6) (2015) 1162–1179. doi:10.1016/j.neuron.2015.08.032.

[5] L. B. Cohen, Changes in neuron structure during action potential propagation and synaptic transmission, Physiological Reviews 53 (2) (1973) 373–418. doi:10.1152/physrev.1973.53.2.373.

[6] T. Heimburg, A. D. Jackson, On soliton propagation in biomembranes and nerves, National Academy of Sciences 102 (28) (2005) 9790–9795. doi:10.1073/pnas.0503823102.

[7] G. H. Kim, P. Kosterin, A. L. Obaid, B. M. Salzberg, A mechanical spike accompanies the action potential in mammalian nerve terminals, Biophysical Journal 92 (2007) 3122–3129. doi:10.1529/biophysj.106.103754.

[8] A. El Hady, B. B. Machta, Mechanical surface waves accompany action potential propagation, Nature Communications 6 (1) (2015) 1–7. doi:10.1038/ncomms7697.

[9] A. Gonzalez-Perez, L. Mosgaard, R. Budvytyte, E. Villagran-Vargas, A. Jackson, T. Heimburg, Solitary electromechanical pulses in lobster neurons, Biophysical Chemistry 216 (2016) 51–59. doi:10.1016/j.bpc.2016.06.005.

[10] T. Ling, K. C. Boyle, V. Zuckerman, T. Flores, C. Ramakrishnan, K. Deisseroth, D. Palanker, High-speed interferometric imaging reveals dynamics of neuronal deformation during the action potential, PNAS 117 (19). doi:10.6084/m9.figshare.11879334).y.

[11] R. Phillips, T. Ursell, P. Wiggins, P. Sens, Emerging roles for lipids in shaping membrane-protein function, Nature Insight 459 (2009) 379–385. doi:10.1038/nature08147.

[12] A. Jerusalem, Z. Al-Rekabi, H. Chen, A. Ercole, M. Malboubi, M. Tamayo-Elizalde, L. Verhagen, S. Contera, Electrophysiological-mechanical coupling in the neuronal membrane and its role in ultrasound neuromodulation and general anaesthesia, Acta Biomaterialia 97 (2019) 116–140. doi:10.1016/j.actbio.2019.07.041.

[13] F. L. Leite, L. H. C. Mattoso, O. N. Oliveira, P. S. P. Herrmann, The atomic force spectroscopy as a tool to investigate surface forces: Basic principles and applications, 2007, pp. 747–757. doi:10.1.1.571.8452.

[14] C. M. Buffinton, K. J. Tong, R. A. Blaho, E. M. Buffinton, D. M. Ebenstein, Comparison of mechanical testing methods for biomaterials: Pipette aspiration, nanoindentation, and macroscale testing, Journal of the Mechanical Behavior of Biomedical Materials 51 (2015) 367–379. doi:10.1016/j.jmbbm.2015.07.022.

[15] L. Qian, H. Zhao, Nanoindentation of soft biological materials, Micromachines 9 (12) (2018) 654. doi:10.3390/mi9120654.

[16] A. Bartolozzi, F. Viti, S. De Stefano, F. Sbrana, L. Petecchia, P. Gavazzo, M. Vassalli, Development of label-free biophysical markers in osteogenic maturation, Journal of the Mechanical Behavior of Biomedical Materials 103 (2020) 1–8. doi:10.1016/j.jmbbm.2019.103581.

[17] V. Lulevich, T. Zink, H.-Y. Chen, F.-T. Liu, G.-Y. Liu, Cell mechanics using atomic force microscopy-based single-cell compression, Langmuir 22 (19) (2006) 8151–8155. doi:10.1021/la060561p.

[18] N. Guz, M. Dokukin, V. Kalaparthi, I. Sokolov, V. Kalapharti, I. Solokov, If cell mechanics can be described by elastic modulus: Study

of different models and probes used in indentation experiments, Biophysical Journal 107 (2014) 564–575. doi:10.1016/j.bpj.2014.06.033.

[19] A. Beyder, F. Sachs, Electromechanical coupling in the membranes of shaker-transfected HEK cells, PNAS 106 (16) (2009) 6626–6631.

[20] M. Tamayo-Elizalde, H. Chen, M. Malboubi, H. Ye, A. Jerusalem, Action potential alterations induced by single f11 neuronal cell loading, Progress in biophysics and molecular biology 162 (2020) 141–153. doi:https://doi.org/10.1016/j.pbiomolbio.2020.12.003.

[21] P. C. Francel, K. Harris, M. Smith, M. C. Fishman, G. Dawson, R. J. Miller, Neurochemical characteristics of a novel dorsal root ganglion x neuroblastoma hybrid cell line, f-11, Journal of Neurochemistry 48 (5) (1987) 1624–1631. doi:10.1111/j.1471-4159.1987.tb05711.x.

[22] S. Fan, K. Shen, M. Scheideler, S. Crain, F11 neuroblastoma × DRG neuron hybrid cells express inhibitory μ - and δ-opioid receptors which increase voltage-dependent k^+ currents upon activation, Brain Research 590 (1) (1992) 329–333. doi:10.1016/0006-8993(92)91116-V.

[23] P. Wieringa, I. Tonazzini, S. Micera, M. Cecchini, Nanotopography induced contact guidance of the f11 cell line during neuronal differentiation: a neuronal model cell line for tissue scaffold development, Nanotechnology 23 (27) (2012) 275102. doi:10.1088/0957-4484/23/27/275102.

[24] J. Prucha, J. Krusek, I. Dittert, V. Sinica, A. Kadkova, V. Vlachova, Acute exposure to high-induction electromagnetic field affects activity of model peripheral sensory neurons, Journal of Cellular and Molecular Medicine 22 (2) (2017) 1355–1362. doi:10.1111/jcmm.13423.

[25] Y.-B. Lu, K. Franze, G. Seifert, C. Steinhauser, F. Kirchhoff, H. Wolburg, J. Guck, P. Janmey, E.-Q. Wei, J. Kas, A. Reichenbach, Viscoelastic properties of individual glial cells and neurons in the CNS, Proceedings of the National Academy of Sciences 103 (47) (2006) 17759–17764. doi:10.1073/pnas.0606150103.

[26] H. Van Hoorn, N. A. Kurniawan, G. H. Koenderink Ac, D. Iannuzzi, Local dynamic mechanical analysis for heterogeneous soft matter using

ferrule-top indentation †, Soft Matter 12 (2016) 3066. doi:10.1039/c6sm00300a.

[27] V. L. Popov, M. Heß, E. Willert, Handbook of Contact Mechanics: Exact Solutions of Axisymmetric Contact Problems, 1st Edition, Springer Berlin Heidelberg, 2019. doi:10.1007/978-3-662-58709-6.

[28] M. Doi, Soft Matter Physics, 1st Edition, Oxford University Press, 2013. doi:10.1093/acprof:oso/9780199652952.001.0001.

[29] J. Seifert, In vivo dynamic AFM mapping of viscoelastic properties of the primary plant cell wall, doctoral (PhD) Thesis, University of Oxford (2018).

[30] L. Bartolini, D. Iannuzzi, G. Mattei, Comparison of frequency and strain-rate domain mechanical characterization, Scientific Reports 8 (1) (2018) 13697. doi:10.1038/s41598-018-31737-3.

[31] M. Malboubi, Y. Gu, K. Jiang, Characterization of surface properties of glass micropipettes using SEM stereoscopic technique, Microelectronic Engineering 88 (8) (2011) 2666–2670. doi:10.1016/j.mee.2011.02.029.

[32] The facts on file dictionary of biology, OCLC: ocm57694687 (2005). doi:10.1093/acref/9780199204625.001.0001.

[33] O. P. Hamill, D. W. Mcbride, Induced membrane hypo/hyper mechanosentitivity: A limitation of patch-clamp recording, Annual Review of Physiology 59 (1997) 621–652. doi:10.1146/annurev.physiol.59.1.621.

[34] A. Magarkar, P. Jurkiewicz, C. Allolio, M. Hof, P. Jungwirth, Increased binding of calcium ions at positively curved phospholipid membranes, The Journal of Physical Chemistry Letters 8 (2) (2017) 518–523. doi:10.1021/acs.jpclett.6b02818.

[35] O. B. Tarun, H. I. Okur, P. Rangamani, S. Roke, Transient domains of ordered water induced by divalent ions lead to lipid membrane curvature fluctuations, Communications Chemistry 3 (1) (2020) 17. doi:10.1038/s42004-020-0263-8.

[36] L. Piantanida, H. L. Bolt, N. Rozatian, S. L. Cobb, K. Voïtchovsky, Ions modulate stress-induced nanotexture in supported fluid lipid bilayers, Biophysical Journal 113 (2) (2017) 426–439. doi:10.1016/j.bpj.2017.05.049.

[37] R. Lipowsky, Remodeling of membrane compartments: some consequences of membrane fluidity, Biological Chemistry 395 (3) (2014) 253–274. doi:10.1515/hsz-2013-0244.

[38] S. O. Yesylevskyy, T. Rivel, C. Ramseyer, The influence of curvature on the properties of the plasma membrane. insights from atomistic molecular dynamics simulations, Scientific Reports 7 (1) (2017) 16078. doi:10.1038/s41598-017-16450-x.

[39] P. Roca-Cusachs, I. Almendros, R. Sunyer, N. Gavara, R. Farré, D. Navajas, Rheology of passive and adhesion-activated neutrophils probed by atomic force microscopy, Biophysical Journal 91 (9) (2006) 3508–3518. doi:10.1529/biophysj.106.088831.

[40] L. Qian, Y. Sun, Q. Tong, J. Tian, Z. Ren, H. Zhao, Indentation response in porcine brain under electric fields, Soft Matter 15 (2019) 623. doi:10.1039/c8sm01272e.

[41] F. Lang, Mechanisms and significance of cell volume regulation, Journal of the American College of Nutrition 26 (2007) 613S–623S. doi:10.1080/07315724.2007.10719667.

[42] J. S. Hub, C. Aponte-Santamaría, H. Grubmüller, B. L. de Groot, Voltage-regulated water flux through aquaporin channels in silico, Biophysical Journal 99 (12) (2010) L97–L99. doi:10.1016/j.bpj.2010.11.003.

[43] K. Takata, T. Matsuzaki, Y. Tajika, Aquaporins: water channel proteins of the cell membrane, Progress in Histochemistry and Cytochemistry 39 (1) (2004) 1–83. doi:10.1016/j.proghi.2004.03.001.

[44] Q. Deng, L. Liu, P. Sharma, Flexoelectricity in soft materials and biological membranes, Journal of the Mechanics and Physics of Solids 62 (2014) 209–227. doi:10.1016/j.jmps.2013.09.021.

[45] S. C. van IJzendoorn, J. Agnetti, A. Gassama-Diagne, Mechanisms behind the polarized distribution of lipids in epithelial cells, Biochimica et Biophysica Acta (BBA) - Biomembranes 1862 (2) (2020) 183145. doi:10.1016/j.bbamem.2019.183145.

[46] M. Jareb, G. Banker, The polarized sorting of membrane proteins expressed in cultured hippocampal neurons using viral vectors, Neuron 20 (5) (1998) 855–867. doi:10.1016/S0896-6273(00)80468-7.

[47] J. Mosbacher, M. Langer, J. Hörber, F. Sachs, Voltage-dependent membrane displacements measured by atomic force microscopy, Journal of General Physiology 111 (1) (1998) 65–74. doi:10.1085/jgp.111.1.65.

[48] K. Xu, G. Zhong, X. Zhuang, Actin, spectrin, and associated proteins form a periodic cytoskeletal structure in axons, Science 339 (6118) (2013) 452–456. doi:10.1126/science.1232251.

[49] E. Fukada, H. Ueda, Piezoelectric effect in muscle, Japanese Journal of Applied Physics 9 (7) (1970) 844–845. doi:10.1143/JJAP.9.844.

[50] I. Ivanov, B. Paarvanova, Dielectric relaxations on erythrocyte membrane as revealed by spectrin denaturation, Bioelectrochemistry 110 (2016) 59–68. doi:10.1016/j.bioelechem.2016.03.007.

[51] R. An, D. O. Wipf, A. R. Minerick, Spatially variant red blood cell crenation in alternating current non-uniform fields, Biomicrofluidics 8 (2) (2014) 021803. doi:10.1063/1.4867557.

[52] E. Fukada, History and recent progress in piezoelectric polymers, IEEE Transactions on Ultrasonics, Ferroelectrics and Frequency Control 47 (6) (2000) 1277–1290. doi:10.1109/58.883516.

[53] H. Athenstaedt, Pyroelectric and piezoelectric properties of vertebrates, Annals of the New York Academy of Sciences 238 (1) (1974) 68–94. doi:10.1111/j.1749-6632.1974.tb26780.x.

[54] B. Machnicka, A. Czogalla, A. Hryniewicz-Jankowska, D. M. Bogusławska, R. Grochowalska, E. Heger, A. F. Sikorski, Spectrins: A structural platform for stabilization and activation of membrane channels, receptors and transporters, Biochimica et Biophysica Acta (BBA) -

Biomembranes 1838 (2) (2014) 620–634. doi:10.1016/j.bbamem.2013.05.002.

[55] M. Bezanilla, A. S. Gladfelter, D. R. Kovar, W.-L. Lee, Cytoskeletal dynamics: A view from the membrane, Journal of Cell Biology 209 (3) (2015) 329–337. doi:10.1083/jcb.201502062.

[56] K. Susuki, M. N. Rasband, Spectrin and ankyrin-based cytoskeletons at polarized domains in myelinated axons, Experimental Biology and Medicine 233 (4) (2008) 394–400. doi:10.3181/0709-MR-243.

[57] B. Stokke, A. Mikkelsen, A. Elgsaeter, Spectrin, human erythrocyte shapes, and mechanochemical properties, Biophysical Journal 49 (1) (1986) 319–327. doi:10.1016/S0006-3495(86)83644-X.

[58] X. Mao, N. Gavara, G. Song, Nuclear mechanics and stem cell differentiation, Stem Cell Reviews and Reports 11 (6) (2015) 804–812. doi:10.1007/s12015-015-9610-z.

[59] N. Wang, J. D. Tytell, D. E. Ingber, Mechanotransduction at a distance: mechanically coupling the extracellular matrix with the nucleus, Nature Reviews Molecular Cell Biology 10 (1) (2009) 75–82. doi:10.1038/nrm2594.

[60] J. Duchesne, J. Depireux, A. Bertinchamps, N. Cornet, J. M. Van Der Kaa, Thermal and electrical properties of nucleic acids and proteins, Nature 188 (1960) 405–406. doi:10.1038/188405a0.

[61] A. Piacenti, Atomic force microscope-based methods for the nanomechanical characterisation of hydrogels and other viscoelastic polymeric materials for biomedical applications, doctoral (PhD) thesis, Universty of Oxford (2021).

[62] J. N. Israelachvili, Intermolecular and surface forces, 3rd Edition, Elsevier, Academic Press, 2011, OCLC: 249272556. doi:https://doi.org/10.1016/C2011-0-05119-0.

[63] K. Gawrisch, A. V. Parsegian, P. R. Rand, Membrane hydration, in: R. Glaser, D. Gingell (Eds.), Biophysics of the Cell Surface, Vol. 5, Springer Berlin Heidelberg, 1990, pp. 61–73, series Title: Springer Series in Biophysics. doi:10.1007/978-3-642-74471-6_5.

[64] W. Trewby, J. Faraudo, K. Voïtchovsky, Long-lived ionic nano-domains can modulate the stiffness of soft interfaces, Nanoscale 11 (10) (2019) 4376–4384. doi:10.1039/C8NR06339G.

[65] S. J. Moe, A. Cembran, Mechanical unfolding of spectrin repeats induces water-molecule ordering, Biophysical Journal 118 (5) (2020) 1076–1089. doi:10.1016/j.bpj.2020.01.005.

[66] X. Li, J. Kolega, Effects of direct current electric fields on cell migration and actin filament distribution in bovine vascular endothelial cells, Journal of Vascular Research 39 (5) (2002) 391–404. doi:10.1159/000064517.

[67] J. Rosenblatt, B. Devereux, D. Wallace, Injectable collagen as a pH-sensitive hydrogel, Biomaterials 15 (12) (1994) 985–995. doi:10.1016/0142-9612(94)90079-5.

[68] J. A. García-Grajales, G. Rucabado, A. García-Dopico, J.-M. Peña, A. Jérusalem, Neurite, a finite difference large scale parallel program for the simulation of electrical signal propagation in neurites under mechanical loading, PLOS ONE 10 (2) (2015) e0116532. doi:10.1371/journal.pone.0116532.

[69] A. Cartagena, A. Raman, Local viscoelastic properties of live cells investigated using dynamic and quasi-static atomic force microscopy methods, Biophysical Journal 106 (5) (2014) 1033–1043. doi:10.1016/j.bpj.2013.12.037.

[70] A. Raman, S. Trigueros, A. Cartagena, A. P. Z. Stevenson, M. Susilo, E. Nauman, S. A. Contera, Mapping nanomechanical properties of live cells using multi-harmonic atomic force microscopy, Nature Nanotechnology 6 (12) (2011) 809–814. doi:10.1038/nnano.2011.186.

[71] R. P. Carney, Y. Astier, T. M. Carney, K. Voïtchovsky, P. H. Jacob Silva, F. Stellacci, Electrical method to quantify nanoparticle interaction with lipid bilayers, ACS Nano 7 (2) (2013) 932–942. doi:10.1021/nn3036304.

[72] Y. Zhang, K. Abiraman, H. Li, D. M. Pierce, A. V. Tzingounis, G. Lykotrafitis, Modeling of the axon membrane skeleton structure and implica-

tions for its mechanical properties, PLoS Computational Biology 13 (2) (2017) e1005407. doi:10.1371/journal.pcbi.1005407.

[73] J. A. Lundbæk, P. Birn, A. J. Hansen, R. Søgaard, C. Nielsen, J. Girshman, M. J. Bruno, S. E. Tape, J. Egebjerg, D. V. Greathouse, G. L. Mattice, R. E. Koeppe, O. S. Andersen, Regulation of sodium channel function by bilayer elasticity, Journal of General Physiology 123 (5) (2004) 599–621. doi:10.1085/jgp.200308996.

[74] J. A. Lundbæk, P. Birn, S. E. Tape, G. E. S. Toombes, R. Søgaard, R. E. Koeppe, S. M. Gruner, A. J. Hansen, O. S. Andersen, Capsaicin regulates voltage-dependent sodium channels by altering lipid bilayer elasticity, Molecular Pharmacology 68 (3) (2005) 680–689. doi:10.1124/mol.105.013573.

[75] D. B. Goldstein, The effect of drugs on membrane fluidity, Annual Review of Pharmacology and Toxicology 24 (1984) 43–64. doi:10.1146/annurev.pa.24.040184.000355.

[76] A. Ievins, C. T. Moritz, Therapeutic stimulation for restoration of function after spinal cord injury, Physiology 32 (5) (2017) 391–398. doi:10.1152/physiol.00010.2017.

[77] C. Moritz, A giant step for spinal cord injury research, Nature Neuroscience 21 (12) (2018) 1647–1648. doi:10.1038/s41593-018-0264-4.

Data availability

Data are available upon request to the corresponding author.